

## Structure and magnetic properties of high coercive NdFeB films with a perpendicular anisotropy

L. K. E. B. Serrona,<sup>a)</sup> A. Sugimura, N. Adachi, T. Okuda,  
H. Ohsato, and I. Sakamoto

*Nagoya Institute of Technology, Gokiso-cho, Showa-ku, Nagoya, 466-8555 Japan*

A. Nakanishi<sup>b)</sup>

*Sumitomo Special Metals Co., Shimamoto-cho, Osaka, 618-0013, Japan*

M. Motokawa

*Institute for Materials Research, Tohoku University, Sendai, 980-8577, Japan*

D. H. Ping and K. Hono

*National Institute for Materials Science, Sengen, Tsukuba 305-0047, Japan*

(Received 16 November 2002; accepted 23 January 2003)

Relatively good hard magnetic properties obtained from Nd<sub>2</sub>Fe<sub>14</sub>B films prepared by the rf sputtering technique were investigated in terms of the microstructural development. Although as-deposited films on Mo substrates deposited at substrate temperatures ( $T_s$ ) of 365 °C were amorphous with the dispersion of nanocrystalline NdO particles, columnar grains of Nd<sub>2</sub>Fe<sub>14</sub>B phase with the  $c$ -axis perpendicular to the film plane developed after annealing at 650 °C at an optimized heating rate. Nd<sub>2</sub>Fe<sub>14</sub>B grain size was about 400 nm in average and NdO particles of about 10 nm were dispersed within the grains and along the grain boundaries. These films exhibited good perpendicular hard magnetic properties of  $iH_c = 1356$  kA/m and  $(BH)_{MAX} \sim 216$  kJ/m<sup>3</sup>. © 2003 American Institute of Physics. [DOI: 10.1063/1.1561576]

Anisotropic high-energy-product Nd<sub>2</sub>Fe<sub>14</sub>B magnetic thin films are the focus of intense interest because of their outstanding potentials for micromagnetic device applications.<sup>1,2</sup> Since the sputter-controlled crystallization process of Nd<sub>2</sub>Fe<sub>14</sub>B thin films led to high coercivity and  $c$  axis crystalline texture,<sup>3</sup> several studies were made to achieve excellent anisotropic behavior, higher coercivity, and better saturation polarization.<sup>4,5</sup> In the postdeposition annealing process, it has been necessary to optimize both the sputtering and thermal annealing conditions separately in order to optimize the transformation of the amorphous Nd–Fe–B phase to a magnetically anisotropic crystalline Nd<sub>2</sub>Fe<sub>14</sub>B phase ( $\Phi$  phase). One of the key factors revealed by a few previous investigations is the effect of substrate deposition temperature on the weak uniaxial magnetic anisotropy in the amorphous films.<sup>5,6</sup> The existence of weak out-of-plane anisotropy in the soft magnetic phase was reported indicated by the increase in both local and macroscopic anisotropy caused by the predominant location of easy axis magnetization perpendicular to the film plane. Earlier investigations further reported that the appropriate substrate deposition temperature to attain excellent hard magnetic properties is limited within a small range below the crystallization temperature ( $T_{crist}$ ). In our previous investigation, we also found that the weak out-of plane anisotropy gave rise to enhanced magnetic properties in annealed films even without any epitaxial rela-

tionship between the (200) oriented Mo substrate and the as-deposited amorphous Nd–Fe–B film.<sup>7</sup> Recently, Shima *et al.*<sup>8</sup> reported on highly anisotropic thin films with the  $c$  axis columnar growth of the Nd<sub>2</sub>Fe<sub>14</sub>B phase occurred by the crystallization of amorphous Nd–Fe–B phase triggered by the Cr cap layer and these columnar grains did not have any epitaxial relationship with the substrate.

In this letter, we present magnetic and nanostructural characteristics of 2  $\mu$ m Nd–Fe–B as-deposited film deposited at substrate temperatures of 300 °C [low temperature deposition (LTD)] and 365 °C [high temperature deposition (HTD)] and correlate them with the corresponding magnetic properties in the crystallized films. We will demonstrate that weak perpendicular anisotropy in as-deposited film is a potential origin of good crystalline texture and enhanced perpendicular magnetic properties in these crystallized films.

The sputtering and annealing conditions are summarized

TABLE I. Sputtering and annealing conditions.

rf sputtering	
Target	Nd <sub>20</sub> Fe <sub>64</sub> B <sub>16</sub> + (1.5 × 1.5) cm <sup>2</sup> Fe Sheet
Ar pressure	6.7 × 10 <sup>-1</sup> Pa
Substrate temperature	300 °C (LTD), 365 °C (HTD)
Deposition time	1 h
Deposition rate	2 $\mu$ m/h
Oxidation protection coating	Ti ~ 700 Å
Annealing	
Vacuum pressure	6.7 × 10 <sup>-4</sup> Pa
Ramp rate	50 °C/min
Temperature	650 °C
Time	30 min

<sup>a)</sup>On leave from the Department of MSE, University of the Philippines-Diliman, Diliman, Quezon City, 1101 Philippines; electronic mail: leokebs@hotmail.com

<sup>b)</sup>Present address: Takuma National College of Technology, Takuma-cho, Mitoyo-gun, Kagawa 769-1192, Japan.

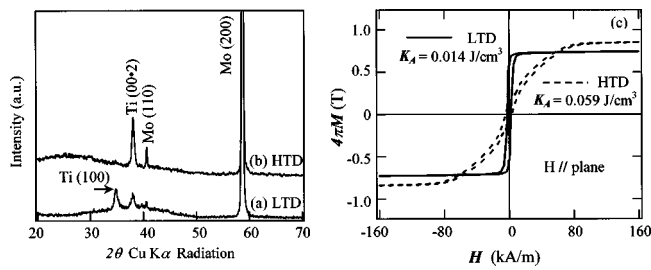


FIG. 1. X-ray diffraction patterns and the corresponding low field part magnetic hysteresis loops for films deposited at (a) 300 °C (LTD mode) and (b) 365 °C (HTD mode).

in Table I. Magnetic and microstructural characterizations were carried out by superconducting quantum interference device (SQUID) and x-ray diffraction (XRD) analysis. Cross-sectional and planar transmission electron microscopy (TEM) observations were also made.

Figures 1(a) and 1(b) show the XRD patterns of as-deposited LTD and HTD films. Both exhibit broad halo pattern, which is the characteristics of the existence of an amorphous structure.

It can be understood that the Ti protective coating crystallized during deposition indicated by the (100) and (00-2) texture both in the LTD and HTD modes. No significant data yet have been established whether this texture has any influence on the microstructure of the as-deposited and annealed films.

Figure 1(c) shows the corresponding low-field part magnetic hysteresis curves of as-deposited films, measured with the magnetic field applied parallel to the film plane. Weak perpendicular anisotropy ( $K_A$ ) in the as-deposited films was estimated by  $K_A = M_s H_s / 2$ , where  $M_s$  is the saturation magnetization value at a point  $H_s$  where the hysteresis curve start to saturate under an applied field.<sup>9</sup>  $K_A$  values estimated for the films deposited at 300 and 365 °C were 0.014 and 0.059 J/cm<sup>3</sup>, respectively. It was reported by Kapitanov *et al.*<sup>5</sup> that the inclination in the loops with respect to the  $4\pi M$ -axis suggests the formation of uniaxial magnetic anisotropy in the magnetically soft state provided that deposition is made within a certain temperature range below the crystallization point of Nd<sub>2</sub>Fe<sub>14</sub>B. Figures 2(a) and 2(b) are TEM planar view images and the corresponding diffraction patterns of the as-deposited films. In both diffraction patterns, no traces of the reflections from the Nd<sub>2</sub>Fe<sub>14</sub>B phase are observed. Figure 2(a) shows that the film is a homogeneous and featureless continuum suggesting a fully amorphous structure. Figure 2(b) is an image for HTD film having small dark spots and long fibrous patterns of crystallized

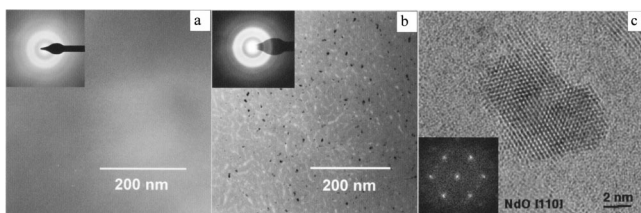


FIG. 2. Planar view bright-field TEM images and corresponding diffraction patterns for films deposited at (a) 300 and (b) 365 °C. (c) High-resolution electron microscope image and the corresponding Fourier transformed electron diffraction pattern of one of the small black NdO particles in Fig. 2(b).

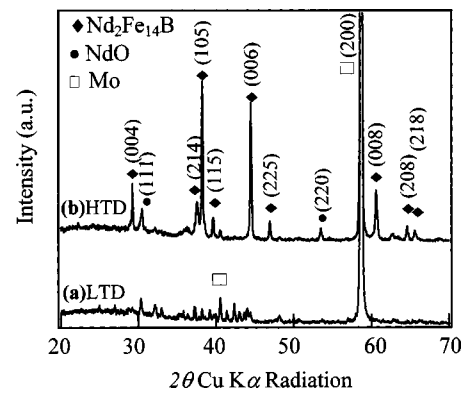


FIG. 3. X-ray diffraction patterns of annealed (a) LTD and (b) HTD films.

particles observed in the amorphous matrix of the film. Shown in Fig. 2(c) is one of these particles identified to be NdO with a fcc structure ( $a \sim 5$  Å) by microbeam diffraction and energy-dispersive x-ray spectroscopy (EDXS). These Nd oxides are believed to have formed during the film deposition. The black and white contrasts of the particles are due to the diffraction contrast from different crystallographic orientation. Observing the cross section TEM image of Fig. 2(b), NdO particles form a thin columnar stacking pattern separating the amorphous phase in a columnar morphology. The tendency to form columnar-like morphology in the as-deposited film is probably associated with the shape anisotropy that caused weak out-of-plane anisotropy. The difference in the  $K_A$  values and the distinction observed in the nanostructure of the as-deposited films may be related to the columnar grain structure formation after crystallization.

The x-ray diffraction patterns of the annealed films are presented in Figs. 3(a) and 3(b). The diffraction pattern of the annealed LTD film reveals the formation of randomly oriented  $\Phi$  phase. For the annealed HTD film, a pronounced texture with the  $c$  axis of the tetragonal  $\Phi$  phase aligned with film normal is observed. The appearance of strong (002 $l$ ) indexes indicates that the crystals of  $\Phi$  phase grew with the  $c$  axis along the film normal. The existence of NdO (111) and (220) is a significant concern because it may cause decrease in the volume fraction of  $\Phi$  phase.

Magnetic hysteresis loops measured parallel and perpendicular to the film plane of the LTD and HTD films are shown in Fig. 4. The LTD film was found to be magnetically isotropic as shown by the nearly similar hysteresis loops in both field directions. Magnetic properties for this isotropic film are  $iH_{c\perp} = 1427$  kA/m,  $4\pi M_{r\perp} = 0.52$  T and obviously low energy-product which cannot be exactly estimated because the loop is not fully saturated even at high fields. In the HTD case, magnetic properties are  $iH_{c\perp} = 1356$  kA/m,  $4\pi M_{r\perp} = 1.06$  T,  $(BH)_{MAX} = 216$  kJ/m<sup>3</sup> and  $M_r/M_s \sim 1$ . The HTD loop was corrected for demagnetizing field with a factor of 0.75. The perpendicular anisotropic properties are consistent with the perpendicular orientation of the  $c$  axis of  $\Phi$  phase.

Figure 5(a) represents a bright-field planar view of a crystallized HTD film. The diffraction pattern obtained from one of the grains is characterized as the [001] zone axis of the Nd<sub>2</sub>Fe<sub>14</sub>B phase. A weak, spotty ring-like pattern in the middle part of the diffraction pattern corresponds to fcc NdO

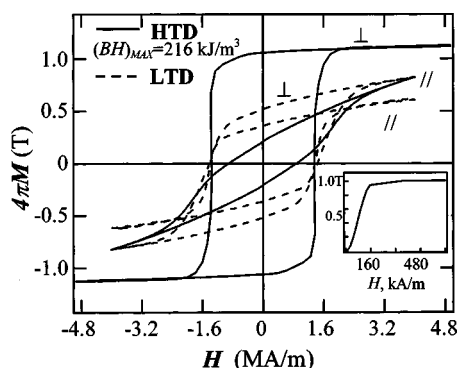


FIG. 4. Magnetic hysteresis loops of annealed LTD and HTD films, for magnetic field directions parallel ( $\parallel$ ) and perpendicular ( $\perp$ ) to the film plane. The nucleation type initial magnetization curve of the film ( $H_{\perp}$  plane) is shown in an inset figure.  $(BH)_{MAX}$  for the HTD film is around  $216 \text{ kJ/m}^3$ .

( $a \sim 5 \text{ \AA}$ ), which are embedded in the matrix grains. As XRD analysis results indicates (Fig. 3), the variation in the volume fraction of NdO against  $\Phi$  phase may also affect the magnetic properties of the films. Figure 5(b) is a bright-field cross-sectional TEM image of the annealed HTD film. As it is clearly seen, a strongly textured columnar grain with an approximate diameter of around  $400 \text{ nm}$  stands vertically on the substrate surface. The diffraction pattern for the columnar grain represents the  $[310]$  zone axis, suggesting that the  $c$  axis is normal the film plane.

The annealed HTD film resulted in a highly  $c$ -axis textured and high-energy-product thin film magnet. Lileev *et al.*<sup>6</sup> pointed out the existence of an isotropy-anisotropy transition at  $340^\circ\text{C} < T_s < 395^\circ\text{C}$ . The result of the present study is consistent with their work, that is HTD sample resulted in high perpendicular coercivity, while LTD sample was rather isotropic. The remarkable magnetic properties of the annealed HTD film can be attributed to the completely crystallized  $\Phi$  phase grains that dominate the entire structure together with a considerable amount of nonmagnetic NdO particles. Although the origin of high coercivity and its mechanism is not yet fully understood, more TEM work is still underway to examine closely the possible cause of the formation of large and columnar grains that is considered to be a major source of perpendicular anisotropy. Planar and cross sectional TEM images in Fig. 5 reveal the presence of a lot of NdO particles both within the grains and along the grain boundaries. Grain boundaries are considerably sharp without any indication of a grain boundary phase. The  $\text{Nd}_{20}\text{Fe}_{64}\text{B}_{16}$  (target composition) phase is Nd and B rich with respect to the stoichiometric composition of the  $\text{Nd}_2\text{Fe}_{14}\text{B}$  phase, thus the formation of NdO is possible. It will remove excess Nd and increase the resultant volume fraction of the  $\text{Nd}_2\text{Fe}_{14}\text{B}$  phase. The excess Nd is transformed into a nanometer-scale distribution of Nd oxides both in the amorphous and annealed state as confirmed by microdiffraction and EDXS investigation. The occurrence of NdO represents oxidation that took place during the HTD deposition and annealing processes. The volume fraction of the oxide phase in the film is considerable, however, these NdO particles seem to play no significant role for magnetic do-

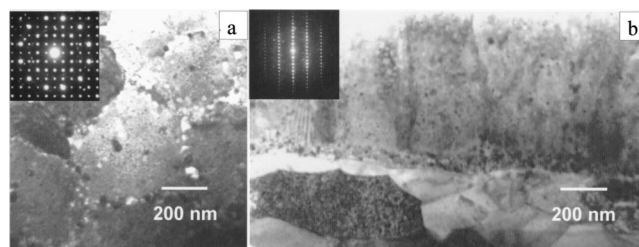


FIG. 5. TEM images of HTD film with corresponding e-beam diffraction patterns: (a) a planar view grain size and (b) cross-sectional view.

main wall pinning. Pinning can correspond to high coercivity in the films but initial magnetization curve of the annealed films is of nucleation type as shown in an inset in Fig. 4.

The Mo substrate used has a surface roughness (rms) of  $\sim 104 \text{ nm}$  and also, due to the nonepitaxial deposition growth of the film, defects and vacancies in the substrate-film interface may occur resulting in a substantial interface stress. Figure 5(b) also shows a thin layer of nanocrystalline particles separating the Mo grains from the homogenous  $\text{Nd}_2\text{Fe}_{14}\text{B}$  grains. During rapid crystallization grain growth, nucleation of the  $\Phi$  phase may have taken place in Nd rich areas enclosed by clustered NdO particles previously deposited from the Nd-B rich target. Nucleation seed particles started to grow at the expense of very fine crystallites to reduce interfacial energy of the system. At the interface, particles remained unaffected due to the difficulty of overcoming defects and internal stresses.

We showed that the presence of weak out-of-plane anisotropy and existence of NdO particles in as-deposited  $\text{NdFeB}$  thin films depend sensitively on  $T_s$ . The as-deposited film grown at  $365^\circ\text{C}$  containing clustered NdO particles yielded a higher effective anisotropy constant of  $0.059 \text{ J/cm}^3$  possibly caused by the shape anisotropy from the columnar-like formation at the cross section of the film. The weak anisotropy resulted to the realization of highly anisotropic and high-energy product thin film after crystallization. TEM observations confirmed the existence of fcc NdO and columnar  $\Phi$  phase grains having nearly single domain size around  $400 \text{ nm}$ . A sharp interface exists between the  $[001]$  oriented  $\text{Nd}_2\text{Fe}_{14}\text{B}$  columnar grain structures.

- <sup>1</sup>T. S. Chin, *J. Magn. Magn. Mater.* **209**, 75 (2000).
- <sup>2</sup>S. Yamashita, J. Yamasaki, M. Ikeda, and N. Iwabuchi, *J. Appl. Phys.* **70**, 6627 (1991).
- <sup>3</sup>F. J. Cadieu, T. D. Cheung, and L. Wickramasekara, *J. Magn. Magn. Mater.* **54–57**, 535 (1986).
- <sup>4</sup>T. Araki, T. Nakanishi, and T. Umemura, *J. Appl. Phys.* **85**, 4877 (1999).
- <sup>5</sup>B. A. Kapitanov, N. V. Kornilov, Ya. L. Linetsky, and V. Yu Tsvetkov, *J. Magn. Magn. Mater.* **127**, 289 (1993).
- <sup>6</sup>A. S. Lileev, A. A. Parilov, and V. G. Blatov, *J. Magn. Magn. Mater.* **242–245**, 1300 (2002).
- <sup>7</sup>L. K. E. B. Serrona, A. Sugimura, R. Fujisaki, T. Okuda, N. Adachi, H. Ohsato, I. Sakamoto, A. Nakanishi, and M. Motokawa, *Trans. Magn. Soc. Jpn.* **2**, 93 (2002).
- <sup>8</sup>T. Shima, A. Kamegawa, K. Hono, and Fujimori, *Appl. Phys. Lett.* **78**, 2049 (2001).
- <sup>9</sup>B. X. Gu, H. Homburg, S. Methfessel, and H. R. Zhai, *Phys. Status Solidi A* **120**, 159 (1990).